

Two-Gaussian excitations model for the glass transition

Dmitry V. Matyushov* and C. A. Angell†

Department of Chemistry and Biochemistry, Arizona State University, PO Box 871604, Tempe, AZ 85287-1604

(Dated: November 10, 2018)

We develop a modified “two-state” model with Gaussian widths for the site energies of both ground and excited states, consistent with expectations for a disordered system. The thermodynamic properties of the system are analyzed in configuration space and found to bridge the gap between simple two state models (“logarithmic” model in configuration space) and the random energy model (“Gaussian” model in configuration space). The Kauzmann singularity given by the random energy model remains for very fragile liquids but is suppressed or eliminated for stronger liquids. The sharp form of constant volume heat capacity found by recent simulations for binary mixed Lennard Jones and soft sphere systems is reproduced by the model, as is the excess entropy and heat capacity of a variety of laboratory systems, strong and fragile. The ideal glass in all cases has a narrow Gaussian, almost invariant among molecular and atomic glassformers, while the excited state Gaussian depends on the system and its width plays a role in the thermodynamic fragility. The model predicts the existence of first-order phase transition for fragile liquids. The analysis of laboratory data for toluene and *o*-terphenyl indicates that fragile liquids resolve the Kauzmann paradox by a first-order transition from supercooled liquid to ideal glass state at a temperature between T_g and Kauzmann temperature extrapolated from experimental data. We stress the importance of the temperature dependence of the energy landscape, predicted by the fluctuation-dissipation theorem, in analyzing the liquid thermodynamics.

I. INTRODUCTION

In the search for understanding of the glass transition phenomenon, attention has been focused overwhelming on the dynamic aspects of the behavior of supercooling liquids.^{1,2,3,4,5,6,7,8,9,10,11,12,13,14} This is natural in view of the general agreement that it is the falling out of equilibrium, at a temperature that depends on the cooling rate, which provokes the observed “drop” in heat capacity at T_g . In other words the glass transition phenomenon observed experimentally is an entirely kinetic phenomenon. However, this approach leaves unresolved a basic thermodynamic question that has troubled glass scientists for the best part of a century.

The thermodynamic problem concerns the course of the entropy in excess of that of the crystal (or any other state whose entropy vanishes at 0 K) during cooling of the equilibrated liquid state. First posed in 1930 by Simon for the particular case of glycerol,¹⁵ and after for a variety of substances by Kauzmann,¹⁶ the question concerns what physical process occurs to avoid the liquid entropy intersecting that of the crystal, as simple extrapolation of the observed entropy changes with decreasing temperature would require for all fragile liquids.¹⁶ Unless it can be shown generally that the liquid becomes mechanically unstable during cooling, (hence has no option but to crystallize), the resolution of this problem requires a thermodynamic description of the liquid entropy which is independent of equilibration time scales. A mechanical instability due to the vanishing of the nucleation bar-

rier was Kauzmann’s resolution¹⁶ of what has become known as the Kauzmann paradox (kinetic phenomenon, T_g , avoiding a thermodynamic crisis, at T_K). Although this resolution has been given recent support from certain crystallizable spin-glass model studies,¹⁷ there is a broad belief that the Kauzmann paradox demands a more general resolution.

While there have been a number of insightful investigations of the thermodynamic properties of glassformers, using the configuration space energy landscape approach,^{18,19,20} there have been surprisingly few attempts to provide theoretical functions to describe the liquid thermodynamics in terms of underlying models. Early attempts were focused on polymers for which quasi-lattice models were plausible. Considering the case of atactic polymers, for which no low energy crystalline state exists, Gibbs and Dimarzio²¹ argued that a thermodynamic (equilibrium) transition of second order, at which the configurational entropy vanishes, must set the limit to supercooling of the liquid state of the polymer. It has been broadly supposed that a similar transition might apply to liquids²² though, without the polymer basis, there is so far less theoretical justification for this. Furthermore, Stillinger²³ has argued that such a transition is not possible in principle, though how closely such a transition could be approached has not been discussed. By contrast, a free volume model by Cohen and Grest⁵ has suggested that, ideally, the transition to the ground state glass should be of first order, though no experimental example has been identified. On the other hand, spin models,⁷ and their application to coarse-grained models of dynamics in structural glasses,^{24,25} have treated the thermodynamic component of the problem as trivial, to be resolved by the thermodynamics of uncorrelated excitations.

*E-mail:dmitrym@asu.edu.

†E-mail:caangell@asu.edu.

Indeed, it has been long known that simple uncorrelated excitation (or defect) models of amorphous solids,^{26,27,28,29} can give a good account of the entropy-temperature relation^{29,30} particularly in elemental cases like selenium.²⁹ These show that the Kauzmann limit paradox can result as a consequence of an unjustified extrapolation of the entropy vs temperature relation, which should be continuous, though rapidly varying, in the vicinity of the Kauzmann temperature. Unfortunately, excitation models in their usual forms (in which the excitations are presumed to be non-interacting), predict the occurrence of a heat capacity maximum above T_g ,^{27,29} which in practice is only found in some strong liquids.^{31,32}

The simple two state model has recently reappeared under a new name, the “logarithmic” model based on its properties in configuration space.³³ Like its real space predecessors, the logarithmic model has the problem of predicting a heat capacity maximum where none is found (though when combined in configuration space with a Gaussian component, this problem is avoided,³³ see below). In a variant of such models, Tanaka^{34,35} has introduced a two order parameter Landau model for the thermodynamics of glassformers where bond length and orientation are distinguished.

A defect model with behavior much like that to be described in this paper (despite a quite different starting point) is the interstitialcy model of Granato.^{36,37} This model posits a single entropy-rich defect (the interstitial defect of crystalline metals) and obtains the temperature dependence of the defect concentration from the temperature dependence of the shear modulus. The cooperativity missing from earlier two state models, or included *ad hoc*,^{27,29} is built in through the proportionality of the defect energy to the shear modulus. The latter decreases strongly with temperature, leading to laboratory-like heat capacities and a phase transition at lower temperatures – which is assigned to a return to the crystal state. Alternatively, Wolynes and co-workers^{38,39} have described a mosaic model in which the inter-domain boundary energies play a vital role in the thermodynamics. With the appropriate assumptions, this model can resolve the Kauzmann paradox in the same way as does the random energy model,^{40,41,42} the system simply running out of states at a singular (Kauzmann) temperature. The sudden, latent heat-free, transition to the ground state is described as a “random first order”

transition,^{38,39} the latent heat of the normal first order transition having been given up continuously over the supercooling temperature range. Both mosaic^{38,39} and constrained excitation^{12,24,25} models prove capable of predicting important dynamic features of glassformers, such as the decoupling of viscosity from diffusivity on approach to the glass transition from above.⁴³ However, in this paper we are concerned only with the thermodynamic problem.

Most theoretical models now gain their support from molecular dynamics computer simulations but, because of their time scale limitations, these cannot be expected to help much with the long time aspects of glass transition problem. The Gaussian distributions of configurational states found in several cases^{44,45,46,47,48,49} in the shorter relaxation time domain (which, however, covers most of the inherent structure energy range between the extrapolated Kauzmann temperature and the high temperature limit) would imply the existence, at lower temperatures, of a Kauzmann-like singularity. Clearly something has to change between the lowest temperature of these simulations and the vanishing entropy temperature, if Stillinger’s argument is to be upheld. In the laboratory behavior of the closest relatives of the most simulated system, binary mixed Lennard-Jones (LJ),^{45,46,48} what changes is the state of the system: it crystallizes, leaving the problem unresolved.

Recent simulation of the thermodynamic behavior of a small periodic box of the mixed soft sphere system by Grigera and Parisi,⁵⁰ Yu and Carruzzo,^{51,52} and De Pablo and co-workers,⁴⁹ suggest, however, that if crystallization does not occur, and equilibrium is maintained, then the heat capacity continues to increase. Finally, it peaks sharply and decreases to zero, like a narrowly avoided Kauzmann singularity. Yan *et al.*⁴⁹ suppose that all possible states of the system have been explored, though this is not yet proven (simulations by Yu and Carruzzo^{51,52} actually indicate that heat capacity drops due to insufficient sampling). In a separate study by Debenedetti and Stillinger,³³ a range of behavior intermediate between the simple two state model and the singularity of the random energy model⁴¹ has been illustrated by adopting, *ad hoc*, an additive mixture of two-state (logarithmic model) and Gaussian (random energy model) distributions. The behavior seen by Yan *et al.*,⁴⁹ and required by experiment,²⁷ is found for Gaussian-rich mixtures.

In the present paper we show how thermodynamic behavior of the sort obtained on soft sphere mixtures^{49,50,51,52} can be reproduced by a modified version of the simple excitations model in which the single (or few) excitation energy(ies) of the original models is(are) replaced by a more physically reasonable Gaussian distribution, the centroid of which may lie near but generally below the value of the original excitation en-

ergy, and the width of which may vary. The existence of such character has been suggested by analysis of spectral band-shapes for glasses and liquids⁵³ and recently, also, the vibrational density of states of glasses of different fictive temperatures in which a quasi-two state behavior is found for the temperature dependence of the vibrational density of states.^{54,55} We note that the Gaussian analysis that is often used to describe the widths of spectral

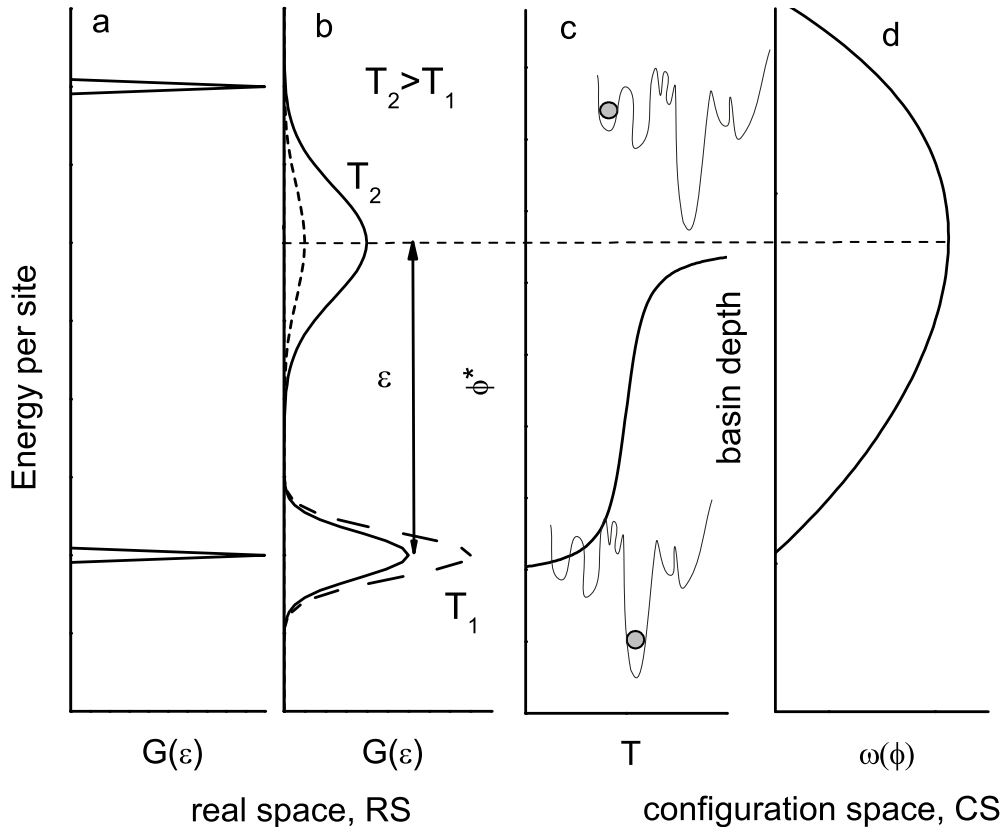


FIG. 1: Real space (RS) energies of perfect crystal sites and defect sites (a). Real space energies and populations of the ideal glass and liquid sites at temperatures $T_1 = T_g$ and T_2 respectively (b). Configuration space (CS) location of system points at $T_1 = T_K$ and T_2 , and the excitation profile (sigmoid) (c). Quasi-Gaussian enumeration function for configurational states (d).

bands, is only appropriate if the modes are localized - which is a poor approximation when dealing with the vibrational density of states, even for the boson peak.⁵⁶ Other spectroscopic evidence for distinct broken bond excitations in glasses has been given for weak network liquids⁵⁷ and recently^{58,59} revived in connection with the boson peak controversy.

II. MODEL REPRESENTATIONS IN REAL SPACE AND CONFIGURATION SPACE (ENERGY LANDSCAPE).

The model assumes the presence in the condensed phase of degrees of freedom which, in real space (RS), can exist in ground (low-energy) and excited (high-energy) states.²⁷ To visualize the model and its relation to crystal defect physics on the one hand, and to energy landscape representations on the other, we use Fig. 1. The distribution of energies in the real space ground state, in the case of the crystal, is a delta function, on the unit

cell length scale, and a small number of delta functions on the per molecule scale (Fig. 1a). The defect states are likewise few in number and well defined in energy. In the glass, however, the sites are not all equivalent on these length scales, and a Gaussian distribution in energy is expected, both for molecules in the ideal glass and for the elementary configurational excitation (or defect) states which we suppose to exist (Fig. 1b). Excitations may be related to coordination defects in covalent materials or to local distortions or packing strains in molecular crystals.

The distribution of energies ϵ_i in real space is characterized by two Gaussians $G_i(\epsilon_i)$ where $i = 1$ stands for the ground state and $i = 2$ stands for the excited state. The Gaussian function $G_i(\epsilon_i)$ is defined by the average ϵ_{0i} and the variance σ_i . In addition to the change in energy, the creation of a local defect may result in an entropy increase related either to a change in the vibrational or configurational density of states.²⁹ The entropy change per molecule of the glass is $s_0 = \Delta S_0/Nk_B$.

The potential energy in configuration space (CS) is a hypersurface depending on all degrees of freedom of the

disordered liquid. The overall configuration space is decomposed into basins of local potential energy minima termed inherent structures.^{23,60} The ideal glass, in configuration space, is represented by the lowest energy basin on the energy landscape, and any excitation of defect states will lift the energy to one or other of the higher energy basins. The more defects in the real space quasi-lattice, the higher the energy of the configuration space basin occupied by the system (Fig. 1c). Thus as the intensity or occupation number of the second real space Gaussian increases (cf. dashed to solid lines in Fig. 1b), the system point in configuration space moves higher on the landscape (Fig. 1c).

The distribution of basin energies (CS) is found, by simulation studies, to conform to a Gaussian (Fig. 1d), but it is barely possible to distinguish between a Gaussian and the binomial distribution that is expected for a two-state system, except at the wings, which are unexplored in any simulations on accessible time scales. The difference must diminish further for the case where the excitation energy is distributed, as in our model. Where a given excitation can occur at any energy in the real space distribution, the states in the configuration space distribution are only occupied on the low energy side of the maximum of the Gaussian (Fig. 1d). The energies in this half Gaussian, though, are uniformly higher than those in the crystal manifold, which is very narrow (Fig. 1c), because the crystal generates very few defects before it becomes thermodynamically unstable and melts.

The density of inherent structures identified with basins of depth ϕ defines the enumeration function $\omega(\phi)$. Following Derrida⁴⁰ and Wolynes,⁶¹ $\omega(\phi)$ can be found by summation over all populations of the excited state

$$e^{N\omega(\phi)} = \sum_{N_2=0}^N C(x) [P(\phi, x)]^{N_2}, \quad (1)$$

where N_2 is the number of excitations out of N molecules in the system, $x = N_2/N$ is the population of the excited state. The function $C(x)$ in Eq. (1) is the number of realizations of a given distribution of molecules between the ground and excited states

$$C(x) = \frac{N!}{(N - N_2)!N_2!} e^{s_0 N_2}. \quad (2)$$

The distribution of basin energies $P(\phi, x)$ in configuration space [Eq. (1)] can be obtained from the real space Gaussians (Fig. 1b),

$$P(\phi, x) = \int \delta(\phi - x\epsilon_2 - (1-x)\epsilon_1) G_2(\epsilon_2) G_1(\epsilon_1) d\epsilon_2 d\epsilon_1. \quad (3)$$

Equation (3) gives a Gaussian distribution of basin energies with the average and variance dependent on the population of excited states in real space

$$P(\phi, x) = [2\pi\sigma]^2 \exp\left[-\frac{(\phi - x\epsilon_0)^2}{2\sigma(x)^2}\right], \quad (4)$$

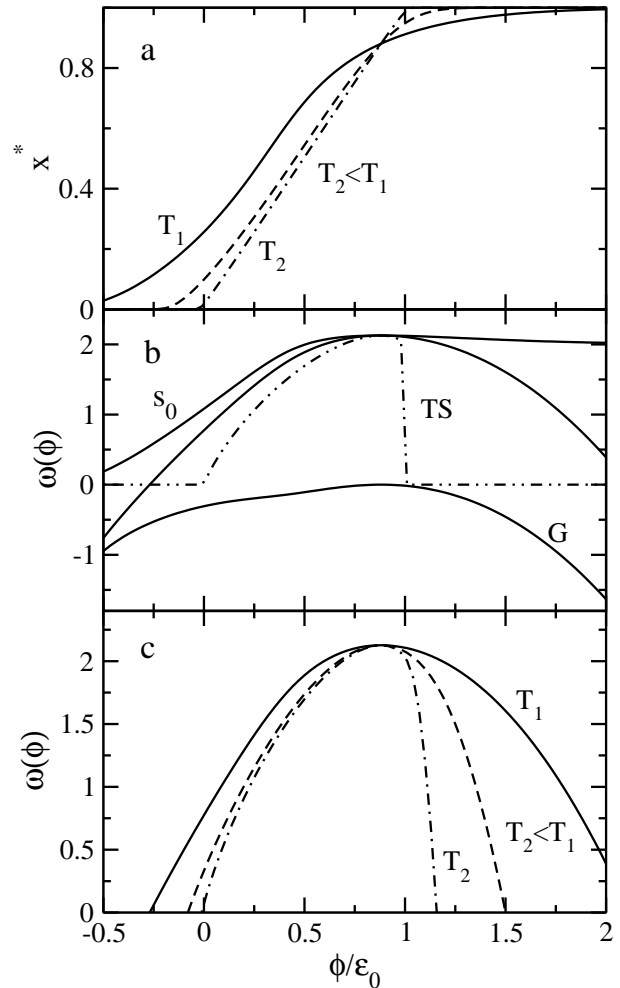


FIG. 2: (a): $x^* = x(\phi^*)$ calculated as the root of Eq. (21). (b) $\omega(\phi)$ from Eq. (10) and its separation into the ideal mixture term “ s_0 ” (first summand in Eq. (10)) and the Gaussian term “ G ” (second summand in Eq. (10)). (c): $\omega(\phi)$ from Eq. (10). The lines in (a)–(c) refer to different temperatures: $T = 500$ K (solid line), $T = 200$ K (dashed line), and $T = 10$ K (dash-dotted line); $\lambda_2/k_B = 200$ K, $\lambda_1/k_B = 100$ K, $\epsilon_0/k_B = 800$ K, $s_0 = 2.0$. The dash-dotted line in (b) shows the enumeration function of the two-state, “TS”, model [Eq. (13)].

where $\epsilon_0 = \epsilon_{02} - \epsilon_{01}$ is the excitation energy and

$$\sigma(x)^2 = (1-x)^2\sigma_1^2 + x^2\sigma_2^2 \quad (5)$$

is the variance of basin energies.

In the thermodynamic limit $N \rightarrow \infty$, the behavior of the sum in Eq. (1) is defined by its largest summand. One finds

$$\omega(\phi) = s(\phi, x(\phi)), \quad (6)$$

where the population at maximum $x(\phi)$ is obtained from the stationary point

$$\left. \frac{ds(\phi, x)}{dx} \right|_{x=x(\phi)} = 0. \quad (7)$$

The function $s(\phi, x) = S(\phi, x)/Nk_B$ is the entropy per molecule at a given population of excited states. From Eqs. (1), (2), and (4) one finds

$$s(\phi, x) = s_0(x) - \frac{(\phi - x\epsilon_0)^2}{2\sigma(x)^2}, \quad (8)$$

where $s_0(x)$ is the entropy of an ideal binary mixture

$$s_0(x) = xs_0 - x \ln x - (1-x) \ln(1-x). \quad (9)$$

The requirement to maximize the entropy at a given basin depth makes the population x a function of ϕ and, therefore, transforms the enumeration function

$$\omega(\phi) = s_0(x(\phi)) - \frac{(\phi - x(\phi)\epsilon_0)^2}{2\sigma(x(\phi))^2} \quad (10)$$

into a generally non-Gaussian dependence on ϕ (Fig. 2). The solution $x(\phi)$ is a root of Eqs. (7) and (8) (Fig. 2a).

In the static energy landscape picture a system at constant volume has a unique energy landscape in the configuration space that is fixed by the intermolecular potential for the particles in the system. From this viewpoint, it seems natural to assume that the variance σ is independent of temperature. If, in addition, the dependence of $x(\phi)$ and $\sigma(\phi)$ on ϕ is neglected in Eq. (10), one arrives at the standard Gaussian model equivalent to the random energy model introduced by Derrida.^{40,41} The Derrida model predicts an ideal glass transition at the Kauzmann temperature $k_B T_K = \sigma/\sqrt{2s_0(x(\phi^*))}$ ($\omega(\phi^*) = 0$ at $T = T_K$) and a hyperbolic temperature dependence of the average basin energy

$$\phi^* = a - b/T. \quad (11)$$

The dependence of the type given by Eq. (11) has indeed been observed in several simulation studies of binary Lennard-Jones (LJ) mixtures,^{48,54} although deviations from this law have also been reported.^{45,47,62,63,64} The heat capacity per molecule $c_V = C_V/Nk_B = k_B^{-1}d\phi^*/dT$ then varies as $c_V \propto 1/T^2$.

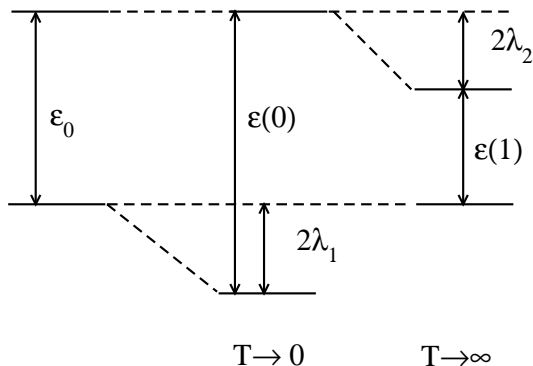


FIG. 3: Temperature dependence of the effective excitation energy $\epsilon(x^*)$ [Eq. (22)]. $\epsilon(0)$ and $\epsilon(1)$ denote the excitation energy at zero and infinite temperature, respectively.

In the limit when the RS Gaussians are much narrower than the excitation energy, $\sigma_i \ll \epsilon_0$, one gets the two-state model.²⁷ The Gaussian term in Eq. (10) then generates a delta function in the density of states $e^{\omega(\phi)}$ requiring $x(\phi) = \phi/\epsilon_0$. This solution also limits the range of accessible basin depths by the condition

$$0 \leq \phi \leq \epsilon_0. \quad (12)$$

The enumeration function in this limit corresponds to the logarithmic energy landscape of Debenedetti, Stillinger, and Shell³³

$$\omega^{\text{TS}}(\phi) = s_0 u - u \ln(u) - (1-u) \ln(1-u), \quad (13)$$

where $u = \phi/\epsilon_0$, $0 \leq u \leq 1$ and the superscript “TS” refers to the two-state model. Note that $s_0 = 0$ is used in the logarithmic model in Ref. 33.

The average basin depth is proportional to the population x_{TS}^* of the RS excited states in the two-state limit:

$$\phi^* = x_{\text{TS}}^* \epsilon_0, \quad x_{\text{TS}}^* = [1 + e^{-s_0 + \beta \epsilon_0}]^{-1}, \quad (14)$$

$\beta = 1/k_B T$. The constant volume heat capacity per particle (in k_B units) is of Schottky’s form^{30,65}

$$c_V^{\text{TS}} = (\beta \epsilon_0)^2 x_{\text{TS}}^* (1 - x_{\text{TS}}^*). \quad (15)$$

This heat capacity form is continuous down to zero K hence, as is well known,^{27,28,29,30} the two-state model eliminates the ideal glass transition ($T_K \rightarrow 0$). Thus variation of the Gaussian width parameters of our model produces the same systematic change of heat capacity form that Debenedetti *et al.*³³ demonstrated by *ad hoc* linear mixing of the Gaussian and binomial distribution CS functions. The heat capacity function for laboratory glasses of different fragility should then reflect the width of the RS Gaussians relative to the separation of their centers.

The present model, which we will refer to as the two-Gaussian (2G) model, projects the two RS Gaussians onto CS enumeration function given by Eq. (10). $\omega(\phi)$ in Eq. (10) is formally a linear combination of the ideal mixture entropy of the RS two-state model and the CS Gaussian term of the Gaussian model. The two terms are connected through the $x(\phi)$ function. $x(\phi)$ is not a linear function of the two-state model [Eq. (14)] when $\sigma_i \neq 0$, although it approaches the linear limit with lowering temperature (Fig. 2a) when RS Gaussians become narrower (see Eq. (20)).

Both the ideal mixture term $s_0(x)$ (first summand in Eq. (10)) and the Gaussian term (second summand in Eq. (10)) are non-parabolic functions of ϕ . A bell-shaped enumeration function, which at high temperatures can be approximated by a Gaussian shape, is a result of combining two non-Gaussian summands in Eq. (10) (Fig. 2b). The two-state limit of the 2G model results in a very asymmetric enumeration function when the excitation entropy s_0 is non-zero due to the cutoff of the range

of accessible basin energies (Eq. (12); dash-dotted line in Fig. 2b).

The connection between the microcanonical entropy $\omega(\phi)$ and the canonical ensemble, which permits calculations at given temperatures, can be obtained by use of two thermodynamic relations⁶⁶

$$\left(\frac{\partial\omega(\phi)}{\partial\phi}\right)_{N,V} = \beta \quad (16)$$

and

$$\left(\frac{\partial^2\omega(\phi)}{\partial\phi^2}\right)_{N,V} = -\frac{\beta^2}{c_V}. \quad (17)$$

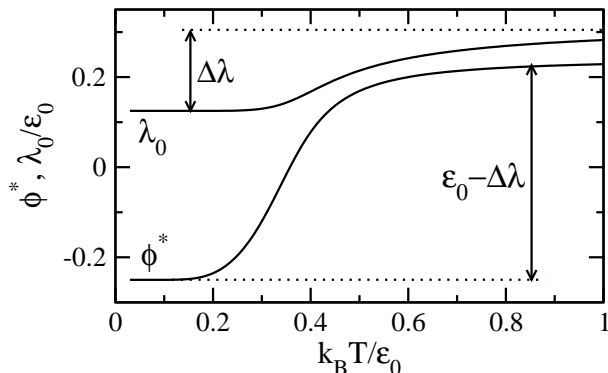


FIG. 4: $\lambda_0(T)$ [Eq. (19)] and ϕ^* [Eqs. (18) and (21)] vs temperature; $\lambda_1/k_B = 100$ K, $\lambda_2/k_B = 200$ K, $\epsilon_0/k_B = 800$ K, $s_0 = 2.0$.

Equation (16) leads to the average energy of inherent structures

$$\phi^* = x^* \epsilon_0 - 2\lambda_0, \quad (18)$$

where $x^* = x(\phi^*)$ and

$$\lambda_0 = (1 - x^*)^2 \lambda_1 + (x^*)^2 \lambda_2. \quad (19)$$

The coupling parameters λ_i in Eq. (19) are defined in terms of the RS distribution widths as

$$\sigma_i^2 = 2k_B T \lambda_i. \quad (20)$$

Equations (5) and (19) immediately lead to Eq. (14) in the limit of narrow RS Gaussians, $\lambda_i \rightarrow 0$. Once Eq. (18) is substituted into Eq. (7), one arrives at a single, self-consistent equation for x^* which is used to obtain the average energy ϕ^* in Eq. (18):

$$x^* = \left[1 + e^{-s_0 + \beta \epsilon(x^*)}\right]^{-1}. \quad (21)$$

Here, $\epsilon(x^*)$ is the population-dependent average excitation energy

$$\epsilon(x^*) = \epsilon_0 - 2x^* \lambda_2 + 2(1 - x^*) \lambda_1. \quad (22)$$

Mechanical stability of the ideal glass state requires

$$\epsilon(x^*) > 0. \quad (23)$$

Equation (21) indicates that the introduction of finite widths to the two RS delta functions of the two-state model results in self-consistency in determining the excited-state population which is governed by the average ground-to-excited energy gap $\epsilon(x)$ [cf. Eqs. (14) and (21)]. The function $\epsilon(x)$ has a simple physical meaning. Going from two states with the gap ϵ_0 to a disordered material with Gaussian distributions of the RS ground and excited state energies makes states with lower random energies thermodynamically more probable. This effectively lowers the energy of each RS state by “solvation” energy $2\lambda_i$ (Stokes shift in spectroscopic applications). The lowering of the energy of each state is, however, scaled with the corresponding population and one gets $2x\lambda_2$ and $2(1-x)\lambda_1$ for lowering the excited and ground states, respectively. The dependence on ground and excited state populations makes the excitation energy decrease with increasing temperature from $\epsilon_0 + 2\lambda_1$ at low temperature to $\epsilon_0 - 2\lambda_2$ at high temperature (Fig. 3).

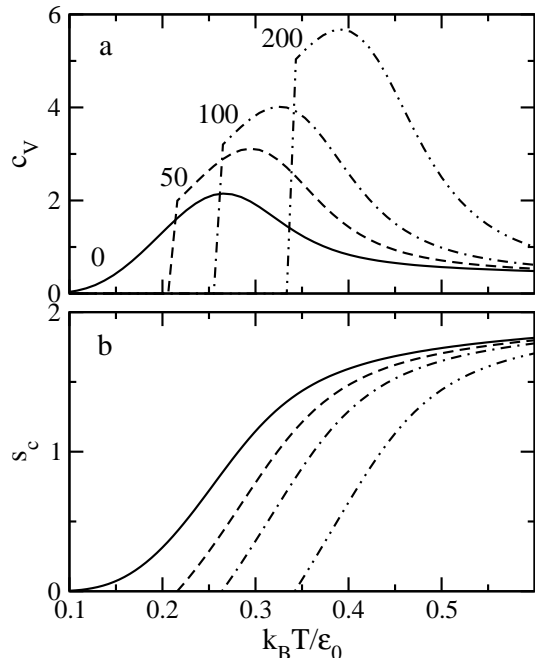


FIG. 5: c_V (a) and s_c (b) (in k_B units) vs temperature at $\lambda_1 = 0$ (solid line), $\lambda_1/k_B = 50$ K (dashed line), $\lambda_1/k_B = 100$ K (dash-dotted line), and $\lambda_1/k_B = 200$ K (dash-double-dotted line); $\lambda_2/k_B = 200$ K, $\epsilon_0/k_B = 800$ K, $s_0 = 2.0$, λ_1 and λ_2 are assumed to be temperature independent. Numbers in plot (a) indicate values of λ_1/k_B .

The second thermodynamic relation [Eq. (17)] allows one to connect the width parameter σ in the CS Gaussian term in Eq. (10) and the constant-volume heat capacity per molecule $c_V(T)$. The width in the Gaussian term can be separated into the $k_B T$ factor and an energetic

coupling parameter related to the RS coupling constants λ_i [Eqs. (19) and (20)]:

$$\sigma^2 = 2k_B T \lambda_0(T), \quad (24)$$

The form of the CS Gaussian width in Eq. (24) is dictated by the classical limit of the fluctuation-dissipation theorem (FDT).⁶⁶ The energy parameter $\lambda_0(T)$ then plays the role of the trapping energy in theories of random-media conductivity⁶⁷ or the solvent reorganization energy in theories of electron transfer.⁶⁸ Alternatively, $\lambda_0(T)$ enters the constant volume heat capacity obtained from Eqs. (10) and (17)

$$c_V(T) = 2\beta\lambda_0(T) [1 - \alpha^*(\epsilon_0 - 4x^*\lambda_2 + 4(1-x^*)\lambda_1)]^{-1}, \quad (25)$$

where

$$\alpha^* = \left. \frac{dx(\phi)}{d\phi} \right|_{\phi=\phi^*}. \quad (26)$$

The separation of the width σ^2 in the $k_B T$ factor and $\lambda_0(T)$ is convenient when the latter is only weakly dependent on temperature. This implies that $c_V(T)$ is approximately a hyperbolic function of temperature $c_V(T) \propto 1/T$ as is empirically documented, at least for the constant pressure heat capacity.^{69,70} The temperature dependence of $\lambda_0(T)$ [Eq. (19)] is determined by the gap $\Delta\lambda = \lambda_2 - \lambda_1$ in the coupling parameters between the ground and excited states since $\lambda_0(T)$ has a sigmoidal form (Fig. 4) with the change $\Delta\lambda$ from low to high temperatures (λ_i are assumed to be temperature independent in Fig. 4). A qualitatively similar sigmoidal form often observed in simulations^{12,71,72,73} is seen for the basin depth ϕ^* . The basin depth increases by the amount $\epsilon_0 - 2\Delta\lambda$ with increasing temperature (Fig. 4).

The description of the glass thermodynamics in terms of a distribution of basin energies involves the projection of the whole configuration space onto a single collective coordinate. This projection onto the lower dimension⁷⁴ introduces a reduced description of the system thermodynamics reflected by the temperature dependence of the moments of the collective coordinate, as is well known from e.g. electron transfer theory.⁶⁸ In fact, thermodynamics [Eq. (17)] and the classical limit of the FDT [Eq. (24)] both predict that, for fluctuations caused by classical motions, σ^2 should decompose into the $k_B T$ factor

and a coupling parameter $\lambda_0(T)$. This is a significant departure from the simple temperature independent behavior of σ^2 supposed to date. Such a temperature dependence modifies predictions of even the simple Gaussian model: no ideal glass transition occurs for temperatures which leave the expression $s_0(x^*) - \beta\lambda_0(T)$ positive. We also note that the combination of disorder with the FDT leads to the excitation energy $\epsilon(x^*)$ [Eq. (22)] decreasing with temperature.

The distribution of basin energies is affected by temperature through the explicit $k_B T$ factor in Eq. (24) and through a more complex temperature variation of $\lambda_0(T)$. Figure 2c shows $\omega(\phi)$ at different temperatures obtained under the assumption that λ_i defined by Eq. (20) are temperature independent. The distribution, which is almost Gaussian at high temperatures, gets skewed from the high-energy wing at lower temperatures (cf. solid and dash-dotted lines in Fig. 2c). The low-energy wing of the enumeration function is not strongly affected by temperature, and low-energy wings at different temperatures can approximately be brought to one master curve by a vertical shift. The high-energy wings differ, however, substantially as temperature changes. Exactly this behavior of the enumeration function curves at different temperatures is reported for the 80-20 LJ binary mixture in Fig. 4 of Ref. 46.

The enumeration function taken at the average basin depth ϕ^* gives the configurational entropy (in k_B units)

$$s_c = s_0(x^*) - \beta\lambda_0. \quad (27)$$

This equation predicts the existence of ideal glass transition, $s_c(T_K) = 0$, at a finite temperature when $\lambda_1 \neq 0$. The Kauzmann temperature T_K tends to zero when $\lambda_1 \rightarrow 0$ and $s_c > 0$ for any $0 < x^* < 1$ at $\lambda_1 = 0$ (solid line in Fig. 5b). The constant volume heat capacity can directly be calculated from Eq. (25). Calculations of $c_V(T)$ at constant λ_2 and varying λ_1 , both temperature independent, are shown in Fig. 5a. At $\lambda_1 \neq 0$ the heat capacity drops to zero at the point of ideal glass transition at $T = T_K > 0$. There is no ideal glass transition when $\lambda_1 = 0$, and the heat capacity passes through a broad maximum.

III. LIQUID-LIQUID(GLASS) FIRST ORDER PHASE TRANSITION

Depending on the value of the excitation entropy s_0 Eq. (21) may have one, two, or three solutions. Only one solution exists for low s_0 since the condition of mechanical stability requires that the effective excitation energy

$\epsilon(x^*)$ remains positive at all excited state populations [Eq. (23)]. Increasing the entropy of excitation allows one to reach the condition of vanishing Gibbs energy of excitation

$$g(x^*) = \epsilon(x^*) - k_B T s_0 \quad (28)$$

TABLE I: Best-fit parameters for model fluids (rows 1-2) and real liquids (rows 3-6). For real liquids, the fitting parameters are λ_1 , λ_2 , ϵ_0 (K) and s_0 are obtained by global fits of Eqs. (22) and (32) to experimental heat capacities and entropies.

Substance	z	T_g	T_{fus}	Δs_{fus}^a	ϵ_0/k_B	λ_1/k_B	λ_2/k_B	s_0^a	T_K^b	T_K^c
80-20 BLJM ^d	1				69.3	8.9	26.5	0.14	34.35 ^e	30.4
50-50 BSSM ^f	1				78.5	2.0	22.3	1.59		14.2
Glycerol	8	190	291	7.55	631	18	32	1.27	136.7	130
Selenium	1	304	494.33	1.50	905	14	27	1.7	210.7	153
Toluene	2	117	178.15	4.48	1045	36	518	5.1	99.9	110 ^g
<i>o</i> -terphenyl	2	246	329.4	6.28	2267	45	1133	5.5	204.1	214 ^g

^aIn k_B units.

^bKauzmann temperature (K) from extrapolation of experimental configurational entropy s_c .

^cKauzmann temperature (K) from the condition $s_c(T_K) = 0$ obtained from the 2G model.

^dBinary LJ A-B mixture with $\epsilon_{AA}/k_B = 119.8$ K, $\epsilon_{AB}/\epsilon_{AA} = 1.5$, $\epsilon_{BB}/\epsilon_{AA} = 0.5$, $\sigma_{BB}/\sigma_{AA} = 0.88$, and density $\rho/\rho_0 = 1.2$, $\rho_0 = 2.5310^{28}$ m³.

^eCalculated from $s_c(T_K) = 0$ in Ref. 48. T_K obtained from the potential energy landscape method is 34.7 K, temperature of vanishing diffusivity from the Vogel-Fulcher-Tammann plot is $T_0 = 35.97$ K.

^fBinary soft sphere mixture. The reduced energy parameters from the fit are multiplied with $\epsilon_{AA}/k_B = 119.8$ K for consistency with the 80-20 BLJM.

^gDetermined as the temperature of the first-order phase transition at which the entropy discontinuously drops to zero.

in the range $0 \leq x^* \leq 1$. At the temperature

$$T_{LL} = (\epsilon_0 - \Delta\lambda)/s_0 \quad (29)$$

the excitation Gibbs energy vanishes at $x^* = 1/2$, $g(1/2) = 0$. This is the temperature of the equilibrium liquid-liquid, first-order phase transition between the low-temperature liquid with low concentration of excitations and the high-temperature liquid with high concentration of excitations.^{75,76} This transition becomes a liquid-glass transition when the low-temperature phase has its viscosity below the glass transition limit or when the transition occurs directly to the ideal glass state.

The first order transition is possible for temperatures below the critical temperature T_c and excitation entropies above the critical value s_{0c} :

$$T < T_c, \quad s_0 > s_{0c}. \quad (30)$$

The critical parameters are

$$\begin{aligned} k_B T_c &= \bar{\lambda} = (\lambda_1 + \lambda_2)/2, \\ s_{0c} &= \frac{\epsilon_0 - \Delta\lambda}{\bar{\lambda}}. \end{aligned} \quad (31)$$

The critical temperature T_c increases and the critical entropy s_{0c} decreases with enhanced disorder of the excited state (Fig. 6). When $T < T_c$ and $s_0 > s_{0c}$, the equilibrium transition temperature, T_{LL} , is flanked by lower, T_l , and upper, T_u , spinodal temperatures at which only two solutions of Eq. (21) are possible: $T_l \leq T_{LL} \leq T_u$ (Fig. 6).

Figure 7 illustrates the change in the temperature variation of the thermodynamic parameters with increasing

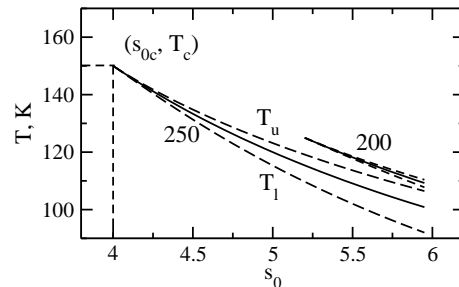


FIG. 6: Equilibrium first-order transition temperature (solid lines) and the lower, T_l , and upper, T_u , spinodal temperatures (dashed lines) vs the excitation entropy s_0 . The calculations are carried out for $\epsilon_0/k_B = 800$ K, $\lambda_1 = 50$ K, and values of λ_2/k_B indicated on the plot; (s_{0c}, T_c) indicates the critical point.

the excitation entropy s_0 . At $s_0 < s_{0c}$, the entropy and basin energy are both continuous functions of temperature. The heat capacity passes through a broad maximum characteristic of the two-state model and drops to zero at a Kauzmann temperature $T_K > 0$ when $\lambda_1 \neq 0$. At the critical excitation entropy $s_0 = s_{0c}$, the entropy and energy both pass through an inflection point reflected by a lambda singularity in the constant volume heat capacity. Finally, the liquid-liquid (glass) phase transition occurs above s_{0c} . The entropy drop at the transition temperature increases with increasing s_0 to the point where the entropy drops to zero. This transition, as well as all transitions with higher entropy s_0 , occur directly from the supercooled liquid to the ideal glass state.

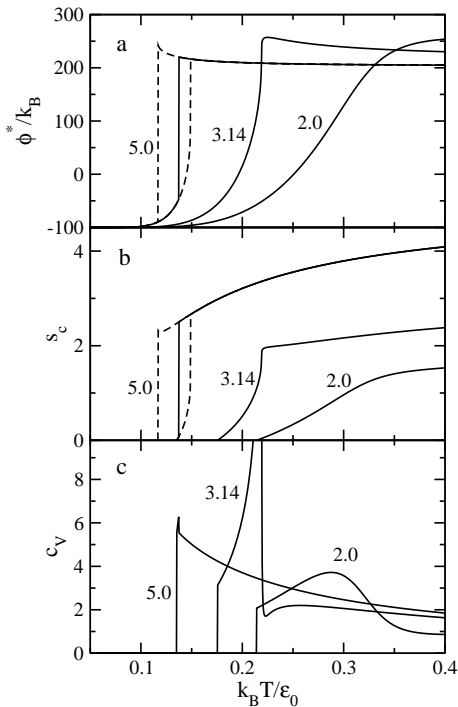


FIG. 7: Basin energy (a), configuration entropy (b), and constant-volume heat capacity (c) at the values of s_0 indicated on the plot; $\lambda_1/k_B = 50$ K, $\lambda_2/k_B = 300$ K, $\epsilon_0/k_B = 800$ K. The values $s_0 = 3.14$ and $k_B T/\epsilon_0 = 0.22$ correspond to the critical point at which lambda singularity for the heat capacity is seen. The dashed lines indicate metastable states between the lower and upper spinodal temperatures.

IV. COMPARISON TO SIMULATIONS

The temperature variation of the energy landscape is critically affected by the approximately linear temperature dependence of the width parameter σ [Eq. (24)] which contributes to the overall temperature variation of the distribution of basin energies

$$P(\phi) \propto e^{\omega(\phi) - \beta\phi}. \quad (32)$$

This generally non-Gaussian distribution is often approximated by a Gaussian function:

$$P(\phi) \propto \exp\left(-\frac{(\phi - \phi^*)^2}{2\Gamma^2}\right) \quad (33)$$

with the empirical Gaussian width Γ . Computer simulations of $P(\phi)$ and the constant volume heat capacity c_V at varying temperature may provide insights into the temperature dependence of σ . Approximately Gaussian distribution of basin energies has been found in simulations of binary LJ^{44,45,46,48} and hard sphere fluids.⁴⁴ Although an increase of the width with temperature is often seen in simulations,^{46,71} numerical data are very limited.

Temperature-dependent width $\Gamma(T)$ can be found in simulations of the well-known 80-20 LJ mixture^{79,80} by

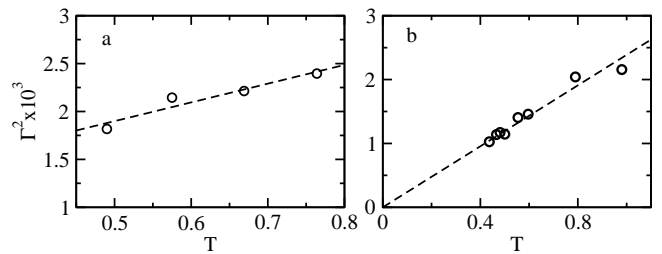


FIG. 8: Variance of the distribution of metabasins in the A-B binary LJ fluid determined from simulations by Denny *et al.*^{77,78} (a) and by Doliwa and Heuer⁷² (b). Units of energy and temperature are defined by the LJ energy of the A-A interaction potential.

Büchner and Heuer.^{45,47} Also, recent extensive simulations by Denny *et al.*⁷⁷ and by Doliwa and Heuer⁷² give the variance of energies of metabasins (basins separated by small minima which do not require activated hops at a given temperature^{72,81}) for the same system at different temperatures. The width of metabasin distribution $\Gamma(T)$ extracted⁷⁸ from the simulations by Denny *et al.*⁷⁷ is approximately linear in T (Fig. 8a). An even steeper $\Gamma(T)$ is found in simulations by Doliwa and Heuer⁷² of the same system of a smaller size (Fig. 8b).

The 2G model is based on four parameters: ϵ_0 , λ_1 , λ_2 , and s_0 . The model is tested on its ability to reproduce several thermodynamic observables for a single set of parameters. We first apply the 2G model to simulations of model fluids and then, in Sec. V, apply it to real liquids. For comparison to computer experiment we fit the average basin energy from 2G model to combined ergodic parts of two cooling runs reported in Ref. 71 for the 80-20 binary LJ mixture (Fig. 9a, Table I). The fitting parameters obtained for the basin depth are used to calculate the configurational entropy [Eq. (27)] which goes to zero (Fig. 9c) at the Kauzmann temperature very close to that obtained from simulations of s_c itself and to T_0 from diffusivity extrapolated to zero through the Vogel-Fulcher-Tammann plot (cf. columns 10 and 11 in Table I).

Since the distribution $P(\phi)$ is generally non-Gaussian, the empirical width Γ was obtained from the half-intensity width of $P(\phi)$. Γ^2 (solid line in Fig. 9b) is larger than σ^2 (dashed line in Fig. 9) since the former reflects the overall width arising from the ideal mixture entropy and the CS Gaussian term in Eq. (10) combined. The empirical width $\Gamma^2(T)$ rises with temperature in accord with the prediction of the FDT and the results of simulations. The magnitude of Γ^2 for the distribution of basins is significantly larger than the one for the distribution of metabasins (cf. Fig. 8 and Fig. 9b). However, the variance of basin energies from MD simulations by Büchner and Heuer^{45,47} (marked “MD” in Fig. 9b) is in reasonable agreement with the 2G model. Finally, the constant volume heat capacity shows a steep rise on approach to the ideal glass transition, dropping to zero at T_K . This

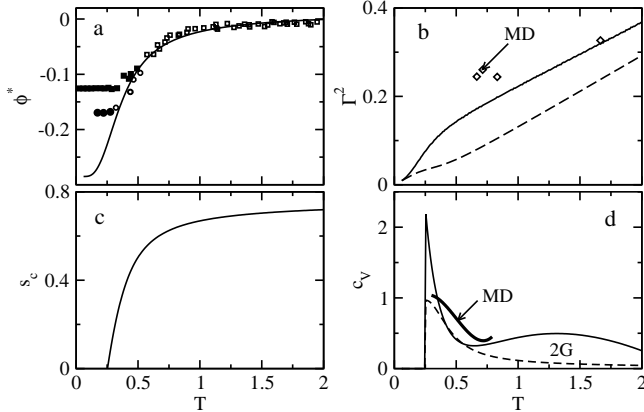


FIG. 9: Inherent structure energy (a), the distribution width (b), configurational entropy (c), and constant volume heat capacity (d) for the 80-20 LJ binary mixture.^{48,71,80} The solid lines refer to calculations with the present model with the parameters obtained from the fit of inherent structure energies from Ref. 71 combining data for the cooling rate $2.7 \cdot 10^{-4}$ (squares) and 3.3310^{-6} (circles). The closed points in (a) indicate the points which were excluded from the fit since they represent the loss of system’s ergodicity due to finite cooling rate. In (b), the solid line refers to Γ^2 , the dashed line refers to σ^2 , and “MD” refers to simulation results for Γ^2 by Büchner and Heuer.^{45,47} In (d), the dashed line refers to the constant P heat capacity calculated under assumption that λ_i are temperature independent. The bold solid line marked “MD” is obtained by numerical differentiation of the configurational entropy from MD simulations by Sciortino *et al.*⁸² and “2G” marks the present model. Units of energy and temperature are defined by the LJ energy of the A-A interaction potential. The parameters of the fit are listed in Table I.

form of the heat capacity is supported by simulations of Sciortino *et al.*⁸² as shown in Fig. 9d. We note that the 80-20 system was originally parameterized to represent the metallic Ni-P alloy⁷⁹ and that metallic glassformers typically show very sharp excess heat capacity functions relative to molecular and ionic glassformers.^{83,84}

A similar fit of the 2G model to the average basin depth of the 50:50 soft sphere (SS) mixture reported by Yan *et al.*⁴⁹ is shown in Fig. 10. The parameters of the fit are used to calculate the distribution width Γ (Eq. (33), Fig. 10b), the configurational entropy (Eq. (27), Fig. 10c), and the constant volume heat capacity (Eq. (25), Fig. 10d). The basin energy width calculated from 2G model ($\Gamma/\epsilon_{AA} = 0.08$) is higher than the one observed in simulations^{51,52} ($\Gamma/\epsilon_{AA} = 0.02$, marked “MD” in Fig. 10b).

Despite the use of parallel tempering MD in Refs. 51 and 52, the drop of the heat capacity at the peak temperature $T_p \simeq 36.5$ K ($\epsilon_{AA}/k_B = 119.8$ K) seen in the simulations is due to insufficient sampling of the phase space.^{51,52} The parameters obtained from the fit of the average basin depth (Table I) give a reasonable description of the simulated $c_V(T)$ up to T_p followed by a much stronger rise of $c_V(T)$ which drops to zero at $T_K \simeq 14$

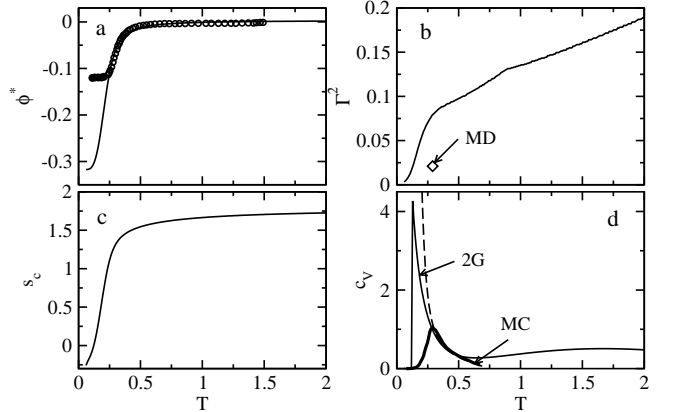


FIG. 10: Same as in Fig. 9 for the 50-50 BSSM studied by Yan *et al.*⁴⁹. The parameters of the fit are listed in Table I. In (b), “MD” marks the Gaussian width from parallel tempering MD simulations reported in Refs. 51 and 52. In (d), “2G” marks the present two-Gaussian model, the bold line marked “MC” refers to the results of Monte Carlo simulations from Ref. 49. The dashed line shows the fit of the c_V simulation data⁵² extrapolated below the temperature of heat capacity drop. The functional form of $c_V(T)$ (dashed line) is from Ref. 52: $c_V(T) = A_1 T^{B_1} + A_2 T^{B_2}$, $A_1 = 2.845$, $B_1 = -0.209$, $A_2 = 3.47710^{-4}$, $B_2 = -5.804$.

K. This latter temperature is close to the point of vanishing configurational heat capacity in the simulations. Note that a peak of $c_V(T)$ higher than the one reported in Refs. 49, 51, and 52 was obtained in MC simulations of analogous binary SS mixture by Grigera and Parisi⁵⁰ within a simulation protocol outperforming parallel tempering. This implies that, once sampling is improved, $c_V(T)$ continues to grow beyond the drop at T_p . Also note that extrapolation of $c_V(T)$ from the fit of simulation data by Yu and Carruzzo⁵² to lower temperatures goes even steeper (dashed line in Fig. 10d) than $c_V(T)$ from 2G model.

V. EXPERIMENTAL CONFIGURATIONAL ENTROPIES AND THE KAUZMANN TEMPERATURE

The configurational heat capacity of a liquid is normally taken as the difference between the liquid and crystal entropies reported for constant pressure, although it is known that in many cases a part of the entropy of fusion is due to an increase in the vibrational entropy (arising from increases in the low frequency vibrational density of states in the liquid inherent structures^{58,73,85}). The constant P configurational heat capacity can be calculated from the configurational entropy in Eq. (27)

$$c_P = T \left(\frac{\partial s_c}{\partial T} \right)_P. \quad (34)$$

The unknown parameter in this calculation is the temperature dependence of the model parameters ϵ_0 , λ_i , and s_0

at constant P . Spectroscopic measurements at constant P give “solvation energies” λ_i through spectral Stokes shifts⁸⁶ which are weakly temperature dependent.⁸⁷ The Stokes shift relates to the coupling of a localized state to a thermal Gaussian bath. Since the defect excitations considered here may be more or less delocalized, it is currently unclear if the assumption $(\partial\lambda_i/\partial T)_P = 0$ is warranted. An alternative scenario might include no temperature dependence of the ideal glass distribution σ_1 corresponding to quenched disorder (i.e., $\lambda_1 \propto 1/T$) and a standard dependence on temperature of σ_2 (i.e., $\lambda_2 = \text{Const}$). It turns out that, when the 2G model is applied to fit the experimental excess heat capacities of the liquid over the crystal, $\Delta c_P = c_{P,\text{liq}} - c_{P,\text{cryst}}$, the results are fairly insensitive to the assumptions made regarding the temperature dependence of λ_1 once the condition $\lambda_2(T) = \text{Const}$ is adopted. The fit of experimental results is thus done with temperature-independent ϵ_0 , λ_i , and s_0 .

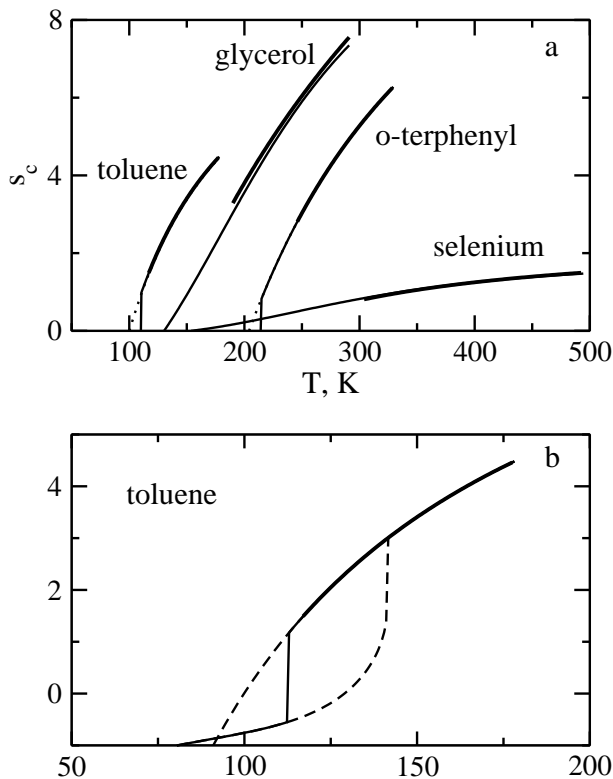


FIG. 11: (a): Configurational entropy s_c vs temperature for liquids listed in Table I. Thick solid lines are experimental results and the thin solid lines are fits to the 2G model. Experimental data stop at the glass transition temperature T_g . Dotted lines show the extrapolation of experimental entropies to the zero entropy line. The fitting parameters are listed in Table I. (b): Temperature dependence of the entropy of toluene (scaled up). The dashed lines indicate the entropies of metastable states terminated at the lower and upper spinodal temperatures.

The fitting procedure involves simultaneous fit of Eqs. (27) and (34) with four fitting parameters, $(\lambda_1, \lambda_2, \epsilon_0,$

and $s_0)$ to experimental heat capacities Δc_P and experimental configurational entropies.³⁰ The range of energy parameters is restricted by the condition of mechanical stability of the ideal glass state [Eq. (23)]. The configurational entropy at constant P can be determined experimentally from the entropy of fusion Δs_{fus} and $\Delta c_P(T)$ (both in k_B units)

$$s_c(T) = \Delta s_{\text{fus}} + \int_{T_{\text{fus}}}^T (\Delta c_P(T')/T') dT'. \quad (35)$$

The 2G model outlined in Sec. II assumes that each molecule represents one excitable unit. While this is true for atomic glasses like selenium, for more complex compounds one needs to introduce the number z of independently excitable (i.e. rearrangeable) states per molecule or formula unit.³⁰ The parameter z is taken from Takeda *et al.*⁸⁸ (Table I) and is used to multiply the heat capacity in Eq. (34) in fitting the experimental data. The results of the fit for four glassformers are listed in Table I.

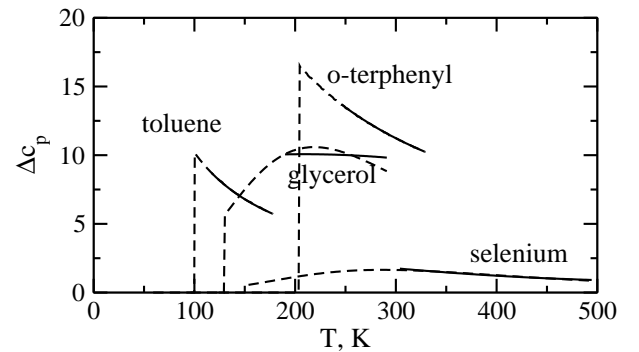


FIG. 12: Comparison of the experimental values of Δc_P (solid lines) with Δc_P calculated from the 2G model (dashed lines) by simultaneous fit to the experimental s_c and Δc_P data above T_g .

The examination of Table I shows that $\lambda_1 > 0$ for all fluid studied, indicating that $T_K > 0$. The distribution of excited states is much narrower in the case of covalent and hydrogen-bonded liquids (selenium and glycerol) compared to molecular liquids (toluene and o-terphenyl). In contrast, the RS distribution of the ideal glass is almost invariant among different glassformers. When $\lambda_2 \gg \lambda_1$ the configurational entropy $s_c(T)$ gains a bend close to the Kauzmann point (Fig. 11) resulting in the actual T_K from $s_c(T_K) = 0$ smaller than the corresponding value from extrapolation of experimental entropies (e.g., selenium in Table I).

The most interesting result of our analysis is the low-temperature behavior of fragile molecular glasses (toluene and o-terphenyl). These substances are characterized by high disorder of the excited state ($\lambda_2 \gg \lambda_1$, Fig. 13) and, in addition, high entropy of excitation (Table I). It also turns out that s_0 from the fit is higher than the critical excitation entropy which is close to 2.0 for both liquids. The fact that s_0 is more than twice

higher than s_{0c} ensures low first-order transition temperature, well below the critical temperature (543 K for toluene and 1156 K for *o*-terphenyl). The first-order transition temperature in fact falls in the unobservable range between T_K and T_g where the entropy discontinuously drops to zero producing a similar drop in the heat capacity (Figs. 11 and 12). It may be therefore suggested that fragile liquids resolve the Kauzmann paradox by a first order liquid-glass transition. We note that both for toluene and *o*-terphenyl the lower spinodal temperature is below the point when metastable entropy crosses the zero entropy line while the upper spinodal temperature is above T_g for toluene and almost coincides with T_g for *o*-terphenyl. Since the first order transition is below T_g , the equilibrium passage along the solid line in Fig. 11b is unlikely thus suggesting hysteresis of the heat capacity between the cooling and heating runs.

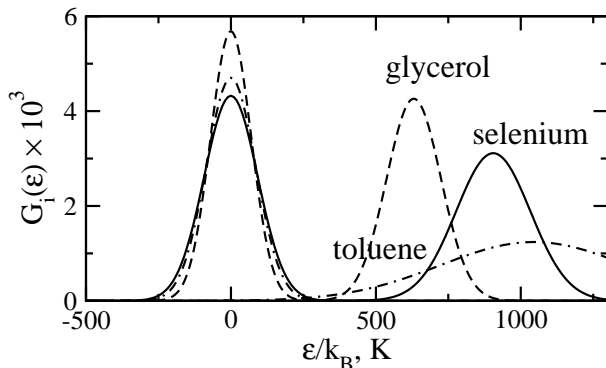


FIG. 13: Real-space distribution of energies for selenium (solid lines), glycerol (dashed lines), and toluene (dash-dotted lines) at their corresponding Kauzmann temperatures. The parameters ϵ_0 and λ_i used in the calculations are taken from Table I.

The value s_0 , which remains an empirical parameter of the 2G model, can be compared to the entropy cost of creating a density wave in density-functional theories of aperiodic structures.^{38,89} The average entropy of the “entropy droplet” in Wolynes’s mosaic model is

$$s_0 = \frac{3}{2} \ln(\alpha r_0^2/\pi) - \frac{5}{2}, \quad (36)$$

where α represents the rms displacement from the lattice site and r_0 is the mean lattice spacing. Invoking the Lindemann ratio³⁸ $\alpha^{1/2}r_0 = 10$, one gets $s_0 = 2.7$, which falls in between entropies for strong and fragile liquids in Table I.

Caution is needed in these interpretations since the model is in the early stages of evaluation and there are four parameters even for simply constituted glasses ($z = 1$). One of these parameters may be disposable. It is apparent from Table I and Fig. 13, that the ground RS Gaussian width best fitting the various data, while non-zero (as expected for a non-crystalline ground state), is small relative to the excited state Gaussian (except

for the stronger liquids) and not varying much between the different systems. It could probably be given a fixed value, reducing the disposable parameters to 3 for simple glasses and 4 for flexible molecule glasses, where the 4th parameter can be fixed from molecular considerations.⁸⁸

VI. CONCLUDING REMARKS

We have shown that by introducing a realistic form for defect-like excitations in glasses, the basic “excitations” model of the glass transition can be developed in a form that bridges the gap between previous over-simple models and the random energy model of Derrida.⁴⁰ In other words, we have provided a physical basis for the previously empirical “logarithmically modified Gaussian” model of Debenedetti *et al.*³³ The model is fundamentally non-Gaussian in configuration space. It recognizes the role of fluctuations within the FDT in making the landscape temperature-dependent as evidenced by the behavior of (meta)basin energy variances from molecular dynamics simulations.^{45,47,51,52,72,77}

The model predicts a possibility of first-order liquid-liquid (glass) transition when the entropy of excitations exceeds its critical value and the temperature falls below the critical point. For fragile liquids characterized by a broad distribution of excitation energies and high entropy change per excitation the transition temperature is low. While most known liquid-liquid transitions for strong liquids are at high temperatures,⁷⁵ the observation of such a transition for fragile supercooled triphenyl phosphite⁷⁶ supports this trend. The fit of the model to experimental entropies and heat capacities of fragile toluene and *o*-terphenyl results in the first-order liquid/ideal glass transition between T_g and the experimental Kauzmann temperature. It seems therefore reasonable to suggest that fragile liquids release the excess entropy by a first-order transition to the glassy state.

The present model belongs to a class of mean-field two-state models in which the average excitation energy drops linearly with the increase in the population of the excited state [Eqs. (21) and (22)]. Negative excitation energies are prohibited by the condition of mechanical stability, and crossing the zero point of the excitation Gibbs energy is driven by the excitation entropy the magnitude of which is correlated with glass fragility.⁹⁰ Another physical realization of this model is the coupling between molecular excited states through long-range interactions. In case of optical excitations of molecules coupled by long-range dipolar forces the change in the excitation energy is realized through the reaction field proportional to the number of excited molecules. A mean-field description, mathematically equivalent to the present 2G model, then results in transition to excitonic condensate in molecules coupled through their transition dipoles⁹¹ or to a non-polar/paraelectric phase transition in dipolar two-state fluids.⁹² In the present model, disorder is responsible for the trapping energy playing the role of the

reaction field in excitonic condensate models.

Acknowledgments

The authors are grateful to Srikanth Sastry and Francesco Sciortino for enlightening discussions and also

to Juan de Pablo and Pablo Debenedetti for helpful comments related to their own work in this area. This work was supported by the NSF through the grants CHE-0304694 (D. V. M.) and DMR0082535 (C. A. A.).

-
- ¹ M. L. Williams, R. F. Landel, and J. D. Ferry, *J. Am. Chem. Soc.* **77**, 3701 (1955).
- ² M. H. Cohen and D. Turnbull, *J. Chem. Phys.* **31**, 1164 (1959).
- ³ D. Turnbull and M. H. Cohen, *J. Chem. Phys.* **34**, 120 (1961).
- ⁴ G. Adam and J. H. Gibbs, *J. Chem. Phys.* **43**, 139 (1965).
- ⁵ M. H. Cohen and G. Grest, *Phys. Rev. B* **20**, 1077 (1979).
- ⁶ M. H. Cohen and G. Grest, *Adv. Chem. Phys.* **48**, 370 (1981).
- ⁷ G. H. Frederickson and H. C. Andersen, *Phys. Rev. Lett.* **53**, 1244 (1984).
- ⁸ W. Götze, in *Liquids, freezing and glass transition*, edited by J. P. Hansen, D. Levesque, and J. Zinn-Justin (Elsevier, Amsterdam, 1991), vol. 1, p. 287.
- ⁹ K. L. Ngai, *J. Chem. Phys.* **98**, 6424 (1993).
- ¹⁰ S. J. Pitts, T. Young, and H. C. Andersen, *J. Chem. Phys.* **113**, 8671 (2000).
- ¹¹ D. N. Perera and P. Harrowell, *J. Chem. Phys.* **111**, 5441 (1999).
- ¹² Y. J. Jung, J. P. Garrahan, and D. Chandler, *Phys. Rev. E* **69**, 061205 (2004).
- ¹³ H. Cang, J. Li, and V. N. N. et al., *J. Chem. Phys.* **118**, 9303 (2003).
- ¹⁴ S. C. Glotzer and C. Donati, *J. Phys.: Condens. Matter* **11**, A285 (1999).
- ¹⁵ F. E. Simon, *Naturwiss.* **9**, 244 (1930).
- ¹⁶ W. Kauzmann, *Chem. Rev.* **43**, 218 (1948).
- ¹⁷ A. Cavagna, I. Giardina, and T. S. Grigera, *J. Chem. Phys.* **118**, 6974 (2003).
- ¹⁸ P. G. Debenedetti, F. H. Stillinger, T. M. Truskett, and C. J. Roberts, *J. Phys. Chem. B* **103**, 7390 (1999).
- ¹⁹ E. L. Nave, S. Mossa, and F. Sciortino, *Phys. Rev. Lett.* **88**, 225701 (2002).
- ²⁰ M. S. Shell, P. G. Debenedetti, E. L. Nave, and F. Sciortino, *J. Chem. Phys.* **118**, 8821 (2003).
- ²¹ J. H. Gibbs and E. A. Dimarzio, *J. Chem. Phys.* **28**, 373 (1958).
- ²² C. A. Angell, *J. Res. NIST* **102**, 171 (1997).
- ²³ F. H. Stillinger, *J. Chem. Phys.* **88**, 7818 (1988).
- ²⁴ J. P. Garrahan and D. Chandler, *Phys. Rev. Lett.* **89**, 035704 (2002).
- ²⁵ J. P. Garrahan and D. Chandler, *Proc. Natl. Acad. Sci. USA* **100**, 9710 (2003).
- ²⁶ P. B. Macedo, W. Capps, and T. A. Litovitz, *J. Chem. Phys.* **44**, 3357 (1966).
- ²⁷ C. A. Angell and K. J. Rao, *J. Chem. Phys.* **57**, 470 (1972).
- ²⁸ J. Perez, *J. Phys. C* **10**, 427 (1985).
- ²⁹ C. A. Angell, *J. Phys.: Condens. Matter* **12**, 6463 (2000).
- ³⁰ C. T. Moynihan and C. A. Angell, *J. Non-Crystal. Sol.* **274**, 131 (2000).
- ³¹ C. A. Angell, E. Williams, K. J. Rao, and J. C. Tucker, *J. Chem. Phys.* **81**, 238 (1977).
- ³² M. Hemmati, C. T. Moynihan, and C. A. Angell, *J. Chem. Phys.* **115**, 6663 (2001).
- ³³ P. G. Debenedetti, F. H. Stillinger, and M. S. Shell, *J. Phys. Chem. B* **107**, 14434 (2003).
- ³⁴ H. Tanaka, *J. Phys.: Condens. Matter* **10**, L207 (1998).
- ³⁵ H. Tanaka, *J. Chem. Phys.* **111**, 3163 (1999), **111**, 3175 (1999).
- ³⁶ A. V. Granato, *Phys. Rev. Lett.* **68**, 974 (1992).
- ³⁷ A. V. Granato, *J. Non-Cryst. Solids* **307-310**, 376 (2002).
- ³⁸ X. Xia and P. G. Wolynes, *Proc. Nat. Acad. Sci.* **97**, 2990 (2000).
- ³⁹ V. Lubchenko and P. G. Wolynes, *J. Chem. Phys.* **121**, 2852 (2004).
- ⁴⁰ B. Derrida, *Phys. Rev. Lett.* **45**, 79 (1980).
- ⁴¹ B. Derrida, *Phys. Rev. B* **24**, 2613 (1981).
- ⁴² R. Richert and H. Bässler, *J. Phys.: Condens. Matter* **2**, 2273 (1990).
- ⁴³ S. F. Swallen, P. A. Bonvallet, R. J. McMahon, and M. D. Ediger, *Phys. Rev. Lett.* **90**, 015901 (2003).
- ⁴⁴ R. J. Speedy and P. G. Debenedetti, *Mol. Phys.* **88**, 1293 (1988).
- ⁴⁵ S. Büchner and A. Heuer, *Phys. Rev. E* **60**, 6507 (1999).
- ⁴⁶ F. Sciortino, W. Kob, and P. Tartaglia, *J. Phys.: Condens. Matter* **12**, 6525 (2000).
- ⁴⁷ A. Heuer and S. Büchner, *J. Phys.: Condens. Matter* **12**, 6535 (2000).
- ⁴⁸ S. Sastry, *Nature* **409**, 164 (2001).
- ⁴⁹ Q. Yan, T. S. Jain, and J. J. de Pablo, *Phys. Rev. Lett.* **92**, 235701 (2004).
- ⁵⁰ T. Grigera and G. Parisi, *Phys. Rev. E* **63** (2001).
- ⁵¹ C. C. Yu and H. M. Carruzzo, cond-mat/0209221.
- ⁵² C. C. Yu and H. M. Carruzzo, *Phys. Rev. E* **69**, 051201 (2004).
- ⁵³ C. A. Angell, in *Vibrational Spectroscopy in Molecular Liquids and Solids*, edited by E. Pick and S. Bratos (Plenum Press, 1980), p. 187.
- ⁵⁴ S. Mossa, E. L. Nave, H. E. Stanley, C. Donati, F. Sciortino, and P. Tartaglia, *Phys. Rev. E* **65**, 041205 (2002).
- ⁵⁵ A. A. Angell, Y. Yue, L.-M. Wang, J. R. D. Copley, S. Borick, and S. Mossa, *J. Phys.: Condens. Matter* **15**, 1 (2003).
- ⁵⁶ V. L. Gurevich, D. A. Parshin, and H. R. Schober, *Phys. Rev. B* **67**, 094203 (2003).
- ⁵⁷ C. A. Angell and J. J. Wong, *J. Chem. Phys.* **53**, 2053 (1970).
- ⁵⁸ C. A. Angell, *J. Phys.: Condens. Matter* **16**, S5153 (2004).
- ⁵⁹ In the case of true networks, the thermodynamics is dominated by the breaking of network bonds^{48,62,63,64} though the observed behavior does not conform to the simple random bond breaking behavior, the broken bonds tending to

- cluster together. Even on the short time scales of molecular dynamics simulations, a completely bonded state can be realized before equilibrium is lost.^{48,62,63,64} However, considerable non-vibrational entropy remains in the amorphous solid, associated with the different manner in which the completely bonded network can be connected.
- ⁶⁰ F. H. Stillinger and T. A. Weber, Phys. Rev. A **25**, 978 (1982).
- ⁶¹ J. D. Bryngelson and P. G. Wolynes, Proc. Natl. Acad. Sci. **84**, 7524 (1987).
- ⁶² I. Saika-Voivod, P. H. Poole, and F. Sciortino, Nature **412**, 514 (2001).
- ⁶³ I. Saika-Voivod, F. Sciortino, and P. H. Poole, Phys. Rev. E **69**, 041503 (2004).
- ⁶⁴ A. Saksengwitt, J. Reinisch, and A. Heuer, Phys. Rev. Lett. **93** (2004).
- ⁶⁵ T. Odagaki, T. Yoshidome, T. Tao, and A. Yoshimori, J. Chem. Phys. **117**, 10151 (2002).
- ⁶⁶ L. D. Landau and E. M. Lifshits, *Statistical physics* (Pergamon Press, New York, 1980).
- ⁶⁷ H. Bässler, Phys. Rev. Lett. **58**, 767 (1987).
- ⁶⁸ R. A. Marcus, Rev. Mod. Phys. **65**, 599 (1993).
- ⁶⁹ Y. Privalko, J. Phys. Chem. **84**, 3307 (1980).
- ⁷⁰ C. Aba, L. E. Busse, D. J. List, and C. A. Angell, J. Chem. Phys. **92**, 617 (1990).
- ⁷¹ S. Sastry, P. G. Debenedetti, and F. H. Stillinger, Nature **393**, 554 (1998).
- ⁷² B. Doliwa and A. Heuer, Phys. Rev. E **67**, 031506 (2003).
- ⁷³ J. Chowdhary and T. Keyes, J. Phys. Chem. B **108**, 19786 (2004).
- ⁷⁴ R. P. Feynman and J. F. L. Vernon, Ann. Phys. **24**, 118 (1963).
- ⁷⁵ S. Sastry and C. A. Angell, Nature Materials **2**, 739 (2003).
- ⁷⁶ H. Tanaka, R. Kurita, and H. Mataka, Phys. Rev. Lett. **92**, 025701 (2004).
- ⁷⁷ R. A. Denny, D. R. Reichman, and J.-P. Bouchaud, Phys. Rev. Lett. **90**, 025503 (2003).
- ⁷⁸ The results presented in Fig. 8 have been extracted from Fig. 2 of Ref. 77. For temperature $T^* = 0.669$, the lowest-energy point substantially deviating from the fit was dropped.
- ⁷⁹ T. A. Weber and F. H. Stillinger, Phys. Rev. B **31**, 1954 (1985).
- ⁸⁰ W. Kob and H. C. Andersen, Phys. Rev. E **51**, 4626 (1995).
- ⁸¹ F. H. Stillinger, Science **267**, 1935 (1995).
- ⁸² F. Sciortino, W. Kob, and P. Tartaglia, Phys. Rev. Lett. **83**, 3214 (1999).
- ⁸³ C. A. Angell, Science **267**, 1924 (1995), see Fig. 1.
- ⁸⁴ R. Busch, J. of Metals **52**, 39 (2000).
- ⁸⁵ M. J. Goldstein, J. Chem. Phys. **64**, 4767 (1976).
- ⁸⁶ R. Richert, J. Chem. Phys. **113**, 8404 (2000).
- ⁸⁷ P. Vath, M. B. Zimmt, D. V. Matyushov, and G. A. Voth, J. Phys. Chem. B **103**, 9130 (1999).
- ⁸⁸ K. Takeda, O. Yamamuro, I. Tsukushi, T. Matsuo, and H. Suga, J. Molec. Struct. **479**, 227 (1999).
- ⁸⁹ C. Dasgupta and O. T. Valls, Phys. Rev. E **59**, 3123 (1999).
- ⁹⁰ C. A. Angell, B. E. Richards, and V. Velikov, J. Phys.: Condens. Matter **11**, A75 (1999).
- ⁹¹ D. E. Logan, J. Chem. Phys. **86**, 234 (1987).
- ⁹² D. V. Matyushov and A. Okhrimovskyy, J. Chem. Phys. **122**, in press (2005).